research articles Journal of proteome research

Proteomic Analysis of Exosomes from Human Neural Stem Cells by Flow Field-Flow Fractionation and Nanoflow Liquid Chromatography−Tandem Mass Spectrometry

Dukjin Kang,[†] Sunok Oh,[†] Sung-Min Ahn,[‡] Bong-Hee Lee,*[,‡] and Myeong Hee Moon*[,†]

Department of Chemistry, Yonsei University, Seoul, 120-749, Korea, and Center for Genomics and Proteomics, Lee Gil Ya Cancer and Diabetes Center, Gachon University of Medicine and Science, Incheon, Korea

Received March 26, 2008

Exosomes, small membrane vesicles secreted by a multitude of cell types, are involved in a wide range of physiological roles such as intercellular communication, membrane exchange between cells, and degradation as an alternative to lysosomes. Because of the small size of exosomes (30−100 nm) and the limitations of common separation procedures including ultracentrifugation and flow cytometry, size-based fractionation of exosomes has been challenging. In this study, we used flow field-flow fractionation (FlFFF) to fractionate exosomes according to differences in hydrodynamic diameter. The exosome fractions collected from FlFFF runs were examined by transmission electron microscopy (TEM) to morphologically confirm their identification as exosomes. Exosomal lysates of each fraction were digested and analyzed using nanoflow LC-ESI-MS-MS for protein identification. FlFFF, coupled with mass spectrometry, allows nanoscale size-based fractionation of exosomes and is more applicable to primary cells and stem cells since it requires much less starting material than conventional gel-based separation, in-gel digestion and the MS-MS method.

Keywords: flow field-flow fractionation • FlFFF • protein separation • exosome • proteomics • nanoflow LC-ESI-MS-MS • mass spectrometry • size separation of exosomes

Introduction

Exosomes are small membrane vesicles (30−100 nm in diameter) secreted by a multitude of cell types as a consequence of the fusion of multivesicular late endosomes/lysosomes with the plasma membrane.[1−3] However, the precise biological functions of exosomes are not fully understood and are dependent on their cell of origin. Although exosomes were first found as a mechanism for shedding membrane proteins such as transferrin receptors during the maturation of reticulocytes,[4] it is now believed that they are involved in a wide range of physiological functions such as intercellular communication, membrane exchange between cells, and as an alternative to lysosomal degradation.[5] Regardless of their putative physiological roles, exosomes also have the potential to be used for cancer immunotherapy. Wolfers and colleagues[6] have suggested that exosomes represent a novel source of tumor-rejection antigens for T-cell cross priming, relevant for immunointervention. In addition, exosomes from dendritic cells (DCs) pulsed with tumor-peptides were able to induce antigen-specific T-cell-mediated immune responses in mice.[7] Also, it was recently reported that, in stem cells, exosomes can deliver not only proteins but also mRNAs, both of which mediate reprogramming of recipient cells.[8]

Exosomes are stable at high temperature with a density range from 1.13 to 1.21 g/mL by density gradient centrifugation (sucrose/D_2O), and can be recognized by expression of a few characteristic proteins (i.e., endocytic markers, tetraspanins and hsp73).[9] The overall size of exosomes has been an important criterion for distinguishing them from other exovesicles, since eukaryotic cells also secrete membrane vesicles directly from the plasma membrane with a mechanism similar to that of viral budding. Membrane vesicles are relatively large and heterogeneous in size ranging from 100 to over 1000 nm.[10] However, it is not easy to analytically distinguish exosomes from membrane vesicles due to the limitations of common separation procedures, including ultracentrifugation and flow cytometry. Heijnen and colleagues[11] used flow cytometry to analyze microvesicles and exosomes released from activated platelets, and found that exosomes were too small to be detected by flow cytometry, thus, making them indistinguishable from microvesicles.

In contrast to flow cytometry, flow field-flow fractionation (FlFFF), an elution-based technique, can separate and characterize macromolecules (e.g., proteins) and nano- to micron-sized particles (e.g., organelles and cells).[12−18] In FlFFF, separation is carried out in a thin and empty rectangular channel with migration flow moving along the channel axis, while sample retention is controlled by the rate of a secondary flow (crossflow in FlFFF) that is applied across the thin channel through a porous channel wall. In the FlFFF channel, there is a balance between the driving force and the diffusion of the particles (see Figure 1 for an enlarged side view). The crossflow

* To whom correspondence should be addressed. Myeong Hee Moon, Department of Chemistry, Yonsei University, Seoul, 120-749, South Korea. Phone, 82 2 2123 5634; fax, 82 2 364 7050; e-mail, mhmoon@yonsei.ac.kr.
[†] Yonsei University.
[‡] Gachon University of Medicine and Science.

10.1021/pr800225z CCC: $40.75

Published on Web 06/21/2008

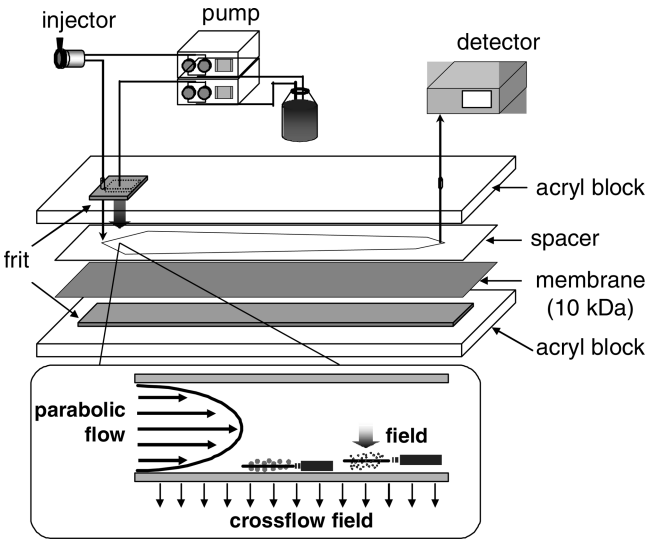

Figure 1. Configuration of the FI-AFlFFF channel with an enlarged side view of the channel indicating the parabolic flow velocity profiles and equilibrium positions of sample components experiencing two opposite forces (crossflow field and diffusion).

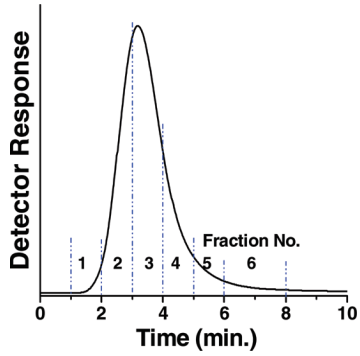

Figure 2. A fractogram of exosomes derived from HB1.F3 cells was obtained by a FFF run. The flow rate conditions for separation of exosomal nanovesicles used were injection flow/frit flow rate = 0.1/2.0 mL/min and sample outflow rate = 45 μL/min, respectively. Fractionated exosomal vesicles were collected at time intervals of 1 min, except fraction 6, which was collected at 2 min.

movement works as an external field to drive sample components toward the channel wall. When an external field is applied, the sample components are differentially distributed against the channel wall due to particle diffusion, and thus, the smaller particles form a distribution layer with a higher mean elevation above the accumulation wall than larger ones. When migration flow is initiated in a channel, small particles with a higher mean layer thickness elute earlier than large ones, resulting in separation of particles with increasing diameter.[12,13] FlFFF can also provide a direct measurement of both hydrodynamic size and size distribution of biological particulate materials such as liposomes and lipoproteins based on the theoretical relationship of size with experimental retention.[19–21]

In this study, we used FlFFF for fractionating exosomes obtained from human neural stem cells (HNSC) according to differences in hydrodynamic diameter. Exosomes fractionated during a FlFFF run were collected by size, and the exosome fractions were examined by transmission electron microscopy (TEM) to confirm their morphology. The exosomal lysate of each fraction was digested, and the resulting peptide mixtures were analyzed using nanoflow liquid chromatography/electrospray ionization−tandem mass spectrometry (nanoflow LC-ESI-MS-MS) for protein identification. To our knowledge, this is the first study providing evidence of nanometer-scale, size-based fractionation of exosomes with morphological confirmation and proteomic analysis.

Experimental Section

Cell Culture. HB1.F3 immortalized human neural stem cells (HMSC) were maintained in Dulbecco's modified Eagle's medium (DMEM) (HyClone; Logan, UT) supplemented with 5% fetal bovine serum (FBS), 5% horse serum, and 50 μg/mL gentamicin at 37 °C and 5% CO_2. Serum proteins and antibiotics were obtained from Invitrogen (Carlsbad, CA).

Exosome Isolation. The procedure for exosome isolation was based on the previously described miniscale exosome purification method[22] with slight modifications for subsequent fractionation using FIFFF. When cells reached 60% confluency, the media was changed, and after 48 h, the supernatants were collected. The collected supernatants were centrifuged at 1000*g* for 10 min to remove cell debris. The clarified supernatant was concentrated to a volume of 1−2 mL by centrifugation for 30 min at 1000*g* in a prerinsed 100 kDa MWCO Centricon Plus-80 capsule filter (Millipore; Danvers, MA). Concentrated exosomes were fractionated using FIFFF.

Flow Field-Flow Fractionation (FlFFF). FlFFF separation of the exosome sample was carried out using a miniaturized frit inlet asymmetrical FlFFF (mFI-AFlFFF) channel as illustrated in Figure 1. FI-AFIFFF is a modified form of flow FFF channel for stopless flow separation that was built in-house and reported in earlier studies.[23,24] The channel space was made by cutting a 178 μm thick Mylar spacer in a ribbon-like shape. The tip-to-tip length, L_{tt}, of the mFI-AFlFFF channel was 9.0 cm, while the initial channel breadth of 1.0 cm was decreased to a final 0.3 cm as a trapezoid. The length of the inlet frit measured from the channel inlet to the end of the relaxation segment was 0.7 cm, and was decreased to a final 0.3 cm at the other end of the trapezoid. The length of the inlet frit measured from the channel inlet to the end of the relaxation segment was 1.1 cm. The geometrical void volume of FFF channel was 76.3 μL. At the accumulation wall, a sheet membrane, PLCGC (molecular weight cutoff: 10 kDa) (Millipore Corp.; Danvers, MA), was placed above the frit to keep sample materials from penetrating the wall. A carrier solution [0.1 M PBS (phosphate buffered saline, pH 7.4)] was filtered through a 0.45 μm membrane filter prior to use and was used for FlFFF separation of exosomes. Sample delivery and frit flow to the mFI-AFlFFF channel were performed individually using two identical HPLC pumps (Model 930 from Young-Lin Co., Seoul, Korea). Eluting exosomes were detected using a Model 730 UV detector (Young-Lin Co.; Seoul, Korea) at a wavelength of 280 nm. Varying lengths of capillary tubing were placed after the detector to control the outflow rate of mFI-AFlFFF channel. Eluting exosomes were collected at 1−2 min intervals.

Transmission Electron Microscopy of Exosome Fractions. Exosome fractions (suspended in less than 0.1 mL of PBS) collected during a FlFFF run were fixed by adding 2% (w/v) osmium tetroxide. After 30 min of fixation, the mixtures were dropped onto a carbon grid (300 mesh) that was placed on filter paper to absorb water from the grid. Once dry, specimens were washed twice with water (by natural draining) and dehydrated using a series of methanol solutions (30, 80, and 100%). After the dehydration steps, the specimens were dried and then

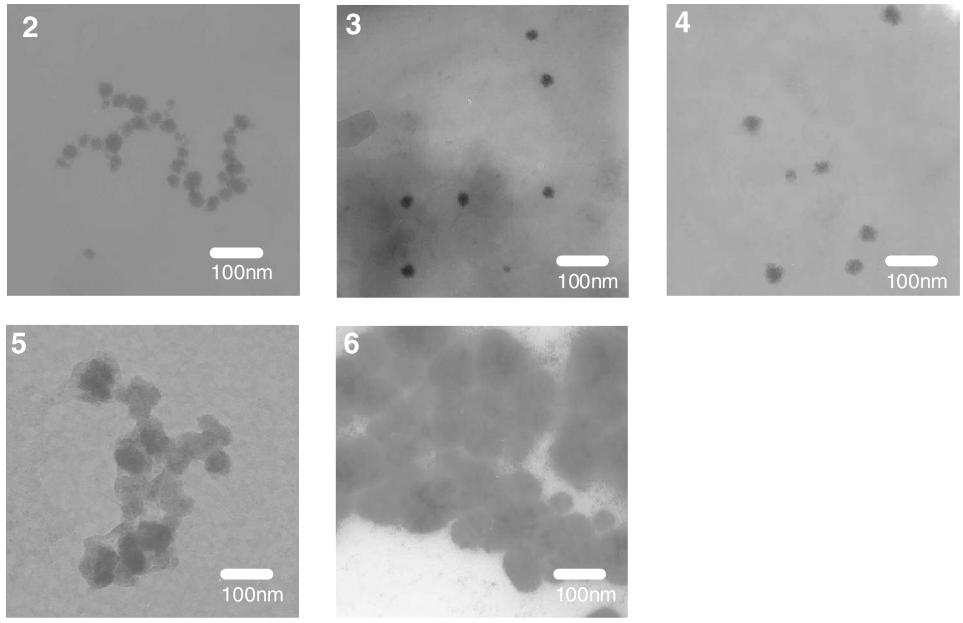

Figure 3. TEM images of each fraction shows morphological changes of exosomal vesicles as a function of their elution time from the FFF channel. Numbers marked in micrographs represent the FFF fraction numbers, respectively.

Table 1. Average Exosome Particle Diameters of Each Fraction Collected During the FlFFF Run

fraction number	time (min)	diameter (nm)	N
2	2.2−3.2	31.6 ± 4.33	17
3	3.2−4.2	34.0 ± 1.40	16
4	4.2−5.2	41.7 ± 4.97	17
5	5.2−6.2	54.0 ± 7.63	10
6	6.2−8.2	101.2 ± 22.4	19

sputtered with gold. Microscopic examination was performed at 5−15 kV of accelerating voltage using a JEM-2000 EXII Transmission Electron Microscopy (JEOL; Tokyo, Japan).

Lysis and In-Solution Digestion of Exosomes. Solution of each exosomal fraction collected during a FlFFF run was exchanged with 0.1 M ammonium bicarbonate solution using an Amicon YM-3 centrifugal filter unit (1 mL) with a 3 kDa molecular mass cutoff membrane filter (Millipore; Bedford, MA) and lysed with tip sonication for 5 min. After lysis, debris were removed by centrifugation at 15 000*g* for 15 min, and supernatants were retrieved for proteomic analysis. For quantification of proteins in each fraction, the Bradford method was utilized.

For shotgun proteomic analysis, each fraction was resuspended in a solution of 8 M urea, 0.01 M NH_4HCO_3 and 10 mM dithiothreitol. After a 2 h incubation, the thiol group was alkylated with iodoacetamide at a total concentration of 20 mM for 2 h at 0 °C in the dark. Excess cysteine (40×) was added to remove excess iodoacetamide, and the resulting mixture was diluted into 1.0 M urea. Proteomics grade trypsin (Sigma; St. Louis, MO) was added at a ratio of 50:1 (trypsin/protein) to the mixture followed by incubation for 18 h at 37 °C. After digestion, tosyl-L-lysyl-chloromethane ketone hydrochloride (TLCK) was added to stop the digestion at a 10:1 molar ratio of TLCK:trypsin. Finally, the digested mixture was desalted using an Oasis HLB cartridge (Waters; Millford, MA), dried, and resuspended in 2% CH_3CN with 0.1% formic acid (FA) for nanoflow LC-ESI-MS-MS analysis.

Nanoflow LC-ESI-MS-MS. Exosomal protein digests (peptide mixtures) of each FlFFF fraction were analyzed by nanoflow LC-ESI-MS-MS using the CapLC system equipped with Q-TOF Ultima mass spectrometer (Waters). A reversed phase capillary LC column (75 μm i.d., 360 μm o.d., 15 cm) was made in the laboratory, and the capillary tip was pulled to a needle using a flame for direct ESI-MS. The pulled-tip column was packed with a methanol slurry of 3 μm, 100 Å Magic C_{18AQ} (Michrom BioResources, Inc.; Auburn, CA) as previously described.[25,26] A trapping column was placed before the analytical column and it was prepared from silica tubing (200 μm i.d., 360 μm

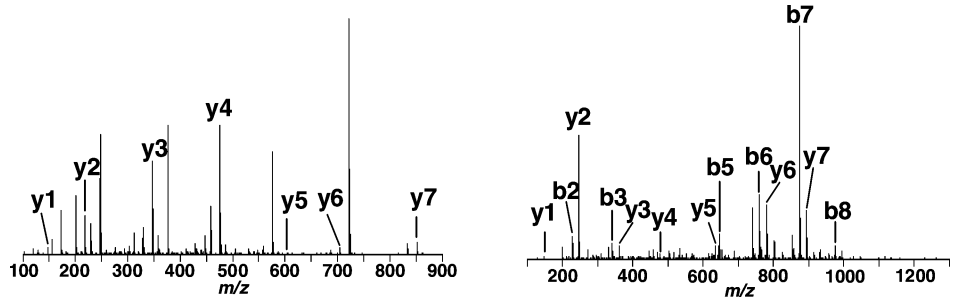

Figure 4. The CID spectra obtained using nLC-ESI-MS-MS of (left panel) the detected peptide ion R.AMTKEEAK.T ($[M + 2H^+]^{2+}$, *m/z* 461.72) from the G protein-coupled receptor associated sorting protein 1 obtained from fraction 2 of FlFFF, and (right panel) K.DLLFRDDTK.C ($[M + 2H^+]^{2+}$, *m/z* 561.79) from the human transferrin receptor-transferrin complex chain F from fraction 3.

Table 2. Identified Proteins by Nanoflow LC-ESI-MS-MS from Exosome Fractions Collected During FIFFF Run Shown in Figure 1

protein name	gi_number	MW	no. of peptides matched	fraction number 2	3	4	5	6
Abhydrolase domain containing 8	gil54611459	47331.4	4	v	v	v	v	v
ADP-ribosylation factor interacting protein 2	gil61359457	37855.7	2	v	v	v		
farnesyltransferase/geranylgeranyltransferase type I alpha subunit	gil51468865	36287.9	1	v	v	v		
G protein-coupled receptor associated sorting protein 1	gil5881845	156865.4	2	v	v	v		v
HIRAHs	gil840774	107034.5	1	v	v	v		
prostaglandin G/H synthase	gil249624	64482.7	1	v	v	v		v
tax1-binding protein TXBP151	gil5776545	86252.1	1	v	v	v		
fenestrated-endothelial linked structure protein	gil12963353	50603.3	1	v	v			v
HLA DR4 antigen beta	gil226424	11330.6	1	v	v			
ankyrin repeat and SOCS box-containing 6	gil55960535	47136.0	5	v		v		
cytochrome P450 2J2	gil18874077	57638.7	3	v		v		
LUZP1 protein	gil30354561	114616.7	1	v		v		
N-ethylmaleimide-sensitive factor attachment protein, gamma	gil12804881	34732.3	2	v		v		
Tetratricopeptide repeat protein 4	gil51475862	44423.9	1	v		v		
aquaporin 5	gil60814784	28292.2	1	v				
CGI-146 protein	gil55665378	11449.1	1	v				
Chain B, Structure Of The Karyopherin Beta2-Ran Gppnhp Nuclear Transport Complex	gil5107636	100821.1	1	v				
Exosome complex exonuclease RRP45	gil14285675	46977.7	2	v				
G protein-coupled receptor kinase GRK4	gil971255	66555.2	1	v				
HSPC090	gil6841120	15479.9	1	v				
MTA1 protein	gil13544098	28705.5	1	v				
MYO1B protein	gil31565495	131985.0	1	v				
NuMA protein	gil35119	238274.5	1	v				
Pex1p-634del690	gil14289171	136584.9	2	v				
rearranged L-myc fusion sequence variant	gil62087778	184694.0	1	v				
synapse associated protein 1	gil57162429	39933.4	1	v				
TAF6-like RNA polymerase II p300	gil46577572	67814.4	1	v				
T-cell ubiquitin ligand protein TULA short form	gil32401083	69790.7	2	v				
thrombospondin-1p180	gil532689	6444.9	2	v				
U3 small nucleolar ribonucleoprotein	gil50355949	88639.0	2	v				
vitamin D-binding protein	gil51863317	24536.0	5	v				
ancient ubiquitous protein AUP1 isoform	gil5410294	53028.3	1		v	v		
ankyrin repeat domain 11 variant	gil62087952	48756.7	1		v	v		
Chain D, Structure Of Pitp-Alpha Complexed To Phosphatidylinositol	gil47169319	31647.4	2		v	v		v
fetuin B	gil61554586	42663.3	2		v	v		
heat shock 70 kDa protein 1A variant	gil62089222	77495.7	2		v	v	v	v
insulin beta chain	gil208660	3430.0	3		v	v		v
Lactoferrin	gil640200	76123.3	1		v	v		
MLEL1 protein	gil11526793	114776.2	1		v	v		
Myotubularin-related protein 2	gil31418327	73354.2	2		v	v		
40S ribosomal protein S16	gil51473203	17940.2	1		v			
Ankyrin repeat and FYVE domain protein 1	gil33514905	128399.2	1		v			
Ca^{2+}-ATPase	gil190099	132722.9	1		v			
cathepsin F precursor	gil6467382	53365.0	2		v			
cyclooxygenase precursor	gil165844	68599.1	1		v			
ezrin	gil5930071	19551.1	1		v			
GREB1a	gil11611734	109076.5	1		v			
Huntingtin interacting protein K	gil51105821	11132.4	2		v			
microcephalin	gil46325253	41939.7	2		v			
nephrocystin 5	gil57230950	68930.1	2		v			
nucleoporin 210-like	gil63501176	96910.3	1		v			
Oligophrenin 1	gil51460447	25662.3	1		v			
Peptidylglycine alpha-amidating monooxygenase COOH-terminal interactor	gil21594849	50020.6	1		v			
PI 3-kinase enhancer long isoform	gil25989575	124673.7	2		v			
polymyositis/scleroderma autoantigen 2	gil56204111	98089.1			v			
receptor-associated coactivator 3	gil2318006	154535.5	1		v			
sarcoma antigen 1	gil51477513	121385.5	1		v			
SFRS7 protein	gil17389794	27366.5	1		v			
SYAP1 protein	gil15779193	39949.5	1		v			
TAK1 binding protein 3	gil37089364	78652.9	1		v			
testis protein TEX14	gil13603885	107238.1	1		v			
UDP-GalNAc:polypeptide *N*-acetylgalactosaminyltransferase	gil1617312	72638.4	1		v			
bromodomain PHD finger transcription factor	gil6683492	311211.7	3			v		
cadherin, EGF LAG seven-pass G-type receptor 2	gil55959329	317452.5	1			v		
caspase recruitment domain protein 11	gil12382773	132642.2	1			v		
CES2 protein	gil48735188	64823.3	1			v		
Chain A, Crystal Structure Of Golgi-Associated Pr-1 Protein	gil55669748	17234.7	1			v		v
Chain A, Solution Structure Of Human Thioltransferase Complex With Glutathione	gil6730102	11580.3	1			v		
Chain F, Structure Of Human Transferrin Receptor-Transferrin Complex	gil48425724	38246.4	1			v		
CHGB	gil5834566	78276.3	1			v		

Table 2. Continued

protein name	gi_number	MW	no. of peptides matched	fraction number 2	3	4	5	6
choline acetyltransferase isoform 2	gi|10181098	82608.9	1			v		
DEK	gi|56417712	42360.9	1			v		
diaphanous homologue 2	gi|57210011	125569.1	1			v		
dishevelled associated activator of morphogenesis 2	gi|40548415	123369.9	1			v		
dynein heavy chain-like protein	gi|55741857	493971.9	1			v		
FYVE-finger-containing Rab5 effector protein Rabenosyn-5	gi|11344951	88801.6	2			v		
golgin-245	gi|1173565	244528.7	1			v		
GTP-binding protein GP-1	gi|7512475	63431.9	3			v		
ITSN1 protein	gi|49257886	74481.2	1			v		
ladinin	gi|2160517	57157.1	2			v		
leucine zipper protein 1	gi|53729365	120304.0	1			v		
MAP/microtubule affinity-regulating kinase 3	gi|46852166	81499.2	1			v		
myosin light chain kinase	gi|30425168	78790.2	1			v		
NUANCE	gi|17016967	796308.3	1			v		
Phosphatidylinositol-4-phosphate 5-kinase	gi|20306910	47327.9	2			v		
Regulating synaptic membrane exocytosis protein 2	gi|41019522	160402.9	1			v		
Rho-related BTB domain-containing protein 3	gi|26006843	69414.4	1			v		
Rho-specific guanine nucleotide exchange factor p114	gi|41327769	114076.7	2			v		
Scaffold attachment factor B2	gi|38372432	107473.4	2			v		
serine/threonine kinase 22C	gi|56203672	30101.9	2			v		
serine/threonine protein kinase kkialre-like 1	gi|18087335	108961.1	1			v		
solute carrier family 35	gi|7960532	39240.1	2			v		
thioredoxin reductase 1	gi|34147767	6584.8	1			v		
thyroid hormone receptor-associated protein complex component TRAP150	gi|4530441	108693.8	1			v		
Translocase of outer mitochondrial membrane 70 homologue A	gi|31419793	67454.8	1			v		
Chain D, Crystal Structure Of Staurosporine Bound To Map Kap Kinase 2	gi|38492557	45329.4	2				v	v
Collagen alpha 2(I) chain precursor	gi|19855162	129455.9	4				v	v
AMBP protein precursor	gi|2506821	39234.8	2				v	
cisplatin resistance associated alpha protein	gi|1688307	27786.7	1				v	
signaling adaptor protein DIP13alpha	gi|16326669	79663.5	3				v	
ADP-ribosylation factor-like protein 4A	gi|41149307	26126.3	2					v
helicase	gi|1517816	101685.7	1					v
Piccolo protein	gi|41019528	566657.1	1					v

o.d.) packed with 5 μm, 200 Å Magic C_{18AQ} to a height of 1 cm. The end frit (2 mm in length) of the trapping column was prepared by sol−gel preparation and was connected via a PEEK Microcross. A platinum (Pt) wire was connected to the microcross to supply the electrospray ionization voltage as described previously.[25,26]

A 1.0 μL sample (about 2 μg for each fraction) of peptide mixture digested from each fraction from FlFFF was loaded onto the trapping column using an autosampler. After sample loading and sufficient desalting with water (0.1% FA), mobile phase solutions (mobile phase composition of (A) 2% CH_3CN in water and (B) 95% CH_3CN in water, both containing 0.1% FA) were delivered to the column, and the effluent was fed into the mass spectrometer via the ESI method. The binary gradient began with 5% B (from 2% B at default) for 5 min, and was increased to 12% B for 25 min, and then to 22% B for 60 min. It was then ramped to 80% B over 3 min, maintained for 10 min for column washing, returned to the default condition over 2 min, and then maintained for at least 25 min for column reconditioning. During the entire run, the column flow rate fed to MS was kept at 200 nL/min. For ESI, a voltage of 2.5 kV at a positive ion mode was applied through the Pt wire. MS analysis of eluted peptides was carried out by a precursor scan (300−1800 amu) followed by three data-dependent MS-MS scans. Collected MS-MS spectra of peptides were analyzed using the Mascot Search program against both Swiss-Prot and NCBI human databases. In screening the search data, only peptides were accepted in case of satisfying the following requirements: (i) the mass tolerances of MS and MS/MS were 1.0 and 0.5 u, respectively; (ii) static modification was set as carbamidomethylation of cysteine including variable modification such as oxidation of methionine; (iii) tryptic enzyme and double miscleavages were defined; and (iv) a minimum Mascot score of above 30 was accepted as an extensive homology.

Results and Discussion

A fractogram of the HNSC exosome sample run was obtained by FlFFF with the following experimental flow rate conditions: injection flow/frit flow = 0.10/2.0 mL/min, outflow rate = 45 μL/min, and crossflow rate = 2.055 mL/min (Figure 2). Since nanosized materials in the FlFFF channel are separated in increasing order of diameter, a broad elution profile indicates that exosomes are of different sizes. While a relatively high speed separation of exosomes was observed (Figure 2), it is not clear how broad the size distribution of exosomes is since the peak broadening (without referring to typical contributions from band broadening sources) is dependent on the flow rate conditions employed for separation. During the FlFFF run, exosomes were collected at intervals of 1 min (except the last fraction which was collected at 2 min) for both microscopic examinations and proteomic analysis. For each run, 20 μL of raw exosomal suspension (from preparative centrifugation) was injected into the FlFFF channel, and the collected fractions were accumulated during nine repeated runs. The exosomes collected in each fraction were analyzed by transmission electron microscope (TEM) (Figure 3). TEM images of each fraction clearly show that FlFFF can fractionate the total exosome population into distinct subpopulations based on their relative sizes. The average diameter of exosomes in each fraction from the TEM images increased as the fraction number increased (Table 1). Interestingly, the shape of the exosomes

appeared to be nearly spherical with only a few elongated specimens. However, the sizes of exosomes in fractions 2−4 are clearly distinguishable from those in fraction 5 and especially from those in fraction 6.

Each exosome fraction from FlFFF was lysed and digested, and the resulting peptide mixtures of each fraction were analyzed by nanoflow LC-ESI-MS-MS. Proteins were identified on the basis of data-dependent CID experiments during nanoflow LC separation. Figure 4, left panel, shows the MS-MS spectra of an ion m/z 461.72 eluted at a retention time of 35.2 min during LC separation of the digests of fraction 2 (the chromatogram is not shown here). This ion was identified as the peptide sequence R.AMTKEEAK.T ($[M + 2H^+]^{2+}$ with a Mascot ion score of 45) that originated from a *G protein-coupled receptor associated sorting protein 1*, which has previously been reported to be an exosomal protein.[27] Likewise, CID spectra of K.DLLFRDDTK.C ($[M + 2H^+]^{2+}$, m/z 561.8, Mascot ion score 51) from *human transferrin receptor-transferrin complex chain F*, also a known exosomal protein,[5,28] was obtained at retention time = 67.1 min of nLC of fraction 3 (Figure 4, right panel).

Shotgun analysis of the peptide mixtures of each fraction resulted in identification of 103 proteins for the five fractions. Among them, 66 proteins were identified from single peptide of each protein. Each single peptide, however, was accepted in case of satisfying the followings: a minimum Mascot score of above 50 and the detection at least more than 2 times for three repetitive shotgun analyses. The identities of proteins found in each exosome fraction are summarized in Table 2. Proteins such as heat shock 70 kDa, transferrin receptor, HLA DR4, and ezrin, previously reported in other exosome studies,[2] were also identified in our study. Several proteins, including abhydrolase-domain-containing-8, G protein-coupled receptor associated sorting protein 1, the 70 kDa heat shock protein 1A variant, and prostaglandin G/H synthase, were present in most fractions, whereas proteins such as cathepsin F precursor and sarcoma antigen 1 were each present in only one fraction.

One of the most intriguing findings of this study was the presence of polymyositis/scleroderma autoantigen 2 (PM/Scl 2), one of the highly specific nuclear autoantigens associated with systemic sclerosis (scleroderma),[29] in exosomes. Exactly how an immune reaction against nuclear proteins in systemic sclerosis is raised has remained elusive, although molecular mimicry between exogenous antigens (e.g., viral proteins) and endogenous antigens has been proposed as a potential cause.[30] As tumor-derived exosomes deliver tumor-rejection antigens and trigger immune reactions,[31] the presence of potential nuclear autoantigens in exosomes indicate that exosomes may be involved in triggering autoimmunity.

Conclusion

Here, we have shown that FIFFF can be successfully used for nanoscale size-based fractionation of exosomes, which has resulted in two novel observations. First, the morphological characterization of exosome subpopulations was accomplished using TEM. We found that exosome subpopulations larger than ~50 nm were morphologically distinct from those smaller than ~50 nm. Second, each exosome fraction showed a different protein pattern, which has analytically important implications. Because the relative abundance of each fraction is different (Figure 2), analysis of the total exosome population without fractionation may lead to loss of important information from the relatively less abundant exosome population (e.g., fraction 1 in Figure 2) due to the limited dynamic range of detection. Finally, size fractionation using FIFFF, followed by in-solution digestion and subsequent shotgun proteomic analysis, can be accomplished with much less starting materials than conventional procedures (gel-based separation, in-gel digestion, and the MS/MS method), thus, providing wider applicability to primary cultures and stem cells where cells cannot be cultured on a large scale.

Acknowledgment. This work was supported by the Korea Foundation for the International Cooperation of Science & Technology (KICOS) through a grant provided by the Korean Ministry of Science & Technology (MOST) in K20713000009-07B0100-00910. B.-H.L. acknowledges the grant support (2006-04090) from Korea Science and Engineering Foundation.

References

(1) Denzer, K.; Kleijmeer, M. J.; Heijnen, H. F.; Stoorvogel, W.; Geuze, H. J. *J. Cell Sci.* **2000**, *113*, 3365–3374.
(2) Mears, R.; Craven, R. A.; Hanrahan, S.; Totty, N.; Upton, C.; Young, S. L.; Patel, P.; Selby, P. J.; Banks, R. E. *Proteomics* **2004**, *4*, 4109–4131.
(3) Johnston, R. M.; Adam, M.; Hammond, J. R.; Orr, L.; Turbide, C. *J. Biol. Chem.* **1987**, *262*, 9412–9420.
(4) Johnstone, R. M. The Jeanne Manery-Fisher Memorial Lecture 1991. *Maturation Biol.* **1992**, *70* (3−4), 179–190.
(5) Thery, C.; Zitvogel, L.; Amigorena, S. *Nat. Rev. Immunol.* **2002**, *2* (8), 569–579.
(6) Wolfers, J.; Lozier, A.; Raposo, G. *Nat. Med.* **2001**, *7* (3), 297–303.
(7) Zitvogel, L.; Regnault, A.; Lozier, A. *Nat. Med.* **1998**, *4* (5), 594–600.
(8) Ratajczak, J.; Miekus, K.; Kucia, M.; Zhang, J.; Reca, R.; Dvorak, P.; Ratajczak, M. Z. *Leukemia* **2006**, *20*, 847–856.
(9) Chaput, N.; Taieb, J.; Schartz, N. E.; Andre, F.; Angevin, E.; Zitvogel, L. *Cancer Immunol. Immunother.* **2004**, *53* (3), 234–239.
(10) Vittorelli, M. L. *Curr. Top. Dev. Biol.* **2003**, *54*, 411–432.
(11) Heijnen, H. F.; Schiel, A. E.; Fijnheer, R.; Geuze, H. J.; Sixma, J. J. *Blood* **1999**, *94* (11), 3791–3799.
(12) Giddings, J. C. *Anal. Chem.* **1981**, *53*, 1170A–1175A.
(13) Wahlund, K.-G.; Litzén, A. *J. Chromatogr.* **1989**, *461*, 73–87.
(14) Giddings, J. C. *Science* **1993**, *260*, 1456–1465.
(15) Reschiglian, P.; Zattoni, A.; Roda, B.; Cinque, L.; Mellucci, D.; Min, B. R.; Moon, M. H. *J. Chromatogr., A* **2003**, *985*, 519–529.
(16) Reschiglian, P.; Zattoni, A.; Cinque, L.; Roda, B.; Piaz, F. D.; Roda, A.; Moon, M. H.; Min, B. R. *Anal. Chem.* **2004**, *76*, 2103–2111.
(17) Kang, D.; Moon, M. H. *Anal. Chem.* **2004**, *76*, 3851–3855.
(18) Kang, D.; Moon, M. H. *Anal. Chem.* **2005**, *77*, 4207–4212.
(19) Moon, M. H.; Giddings, J. C. *J. Pharm. Biomed. Sci* **1993**, *11*, 911.
(20) Moon, M. H.; Kim, Y. H.; Park, I. *J. Chromatogr., A* **1998**, *813* (1), 91–100.
(21) Park, I.; Paeng, K.-J.; Yoon, Y.; Song, J.-H.; Moon, M. H. *J. Chromatogr., B.* **2002**, *780*, 415–422.
(22) Lamparski, H. G.; Metha-Damani, A.; Yao, J.-Y.; Patel, S.; Hsu, D.-H.; Ruegg, C.; Pecq, J.-B. *J. Immunol. Methods* **2002**, *270*, 211–226.
(23) Moon, M. H.; Kwon, H. S.; Park, I. *Anal. Chem.* **1997**, *69*, 1436–1440.
(24) Kang, D.; Moon, M. H. *Anal. Chem.* **2004**, *76*, 3851–3855.
(25) Moon, M. H.; Myung, S.; Plasencia, M.; Hildebrand, A.; Clemmer, D. E. *J. Proteome Res.* **2003**, *2*, 589–597.
(26) Kang, D.; Nam, H.; Kim, Y.-S.; Moon, M. H. *J. Chromatogr., A* **2005**, *1070*, 193–200.
(27) Estelles, A.; Sperinde, J.; Roulon, T.; Aguilar, B.; Bonner, C.; LePecq, J.-B.; Delcayre, E. A. *Int. J. Nanomed.* **2007**, *2*, 751–760.
(28) Pan, B.-T.; Teng, K.; Wu, C.; Adam, M.; Johnstone, R. M. *J. Cell Biol.* **1985**, *101*, 942–948.
(29) Senecal, J. L.; Henault, J.; Raymond, Y. *J. Rheumatol.* **2005**, *32*, 1643–1649.
(30) Jimenez, S. A.; Derk, C. T. *Ann. Intern. Med.* **2004**, *140*, 37–50.
(31) Wolfers, J.; Lozier, A.; Raposo, G.; Regnault, A.; Thery, C.; Masurier, C.; Flament, C.; Pouzieux, S.; Faure, F.; Tursz, T.; Angevin, E.; Amigorena, S.; Zitvogel, L. *Nat. Med.* **2001**, *7*, 297–303.

PR800225Z